Int J Adv Manuf Technol (2017) 92:1751–1760
DOI 10.1007/s00170-017-0227-z

ORIGINAL ARTICLE

Effect of local laser surface texturing on tribological performance of injection cam

Zhengyang Kang[1] · **Yonghong Fu**[1] · **Jinghu Ji**[1] · **Julius Caesar Puoza**[1]

Received: 9 October 2016 / Accepted: 26 February 2017 / Published online: 20 March 2017

Abstract The camshaft is a crucial component of an engine's valve train. This paper devotes to the experimental studies of the performance of laser surface textured (LST) camshaft. The first part experiment was carried out on the block-on-ring tester to investigate the tribological behaviors of textured surface in line contact. The area density of the textured dimples was in the range 3–40% with depths 5–24 μm and diameter 70 μm. The friction coefficient and wear tracks were analyzed to confirm the optimum textured patterns. After that, the local LST cams (textured on the lifting region) were further tested in a single-cylinder diesel. It was found that after 300 h durability test at the rated speed and load, the total lifting loss of cams decreased nearly 34.4% in maximum. In addition, the performance of the engine was not affected evidently. The enhanced lubricity and local hardening were two mechanisms for highly promoting the anti-wear property of the LST cams.

Keywords Laser surface texture · Injection cam · Anti-wear · Nonconformal contact

✉ Zhengyang Kang
kzy_blue@yeah.net

Yonghong Fu
fyh@ujs.edu.cn

Jinghu Ji
jijinghu@ujs.edu.cn

Julius Caesar Puoza
deokaesar@yahoo.co.uk

[1] School of mechanical engineering, Jiangsu University, Zhenjiang, Jiangsu 212013, China

1 Introduction

The cam-roller component has an appreciable impact on the oil and air accurate supplies of the internal combustion engine. For the cam surface, the excellent anti-wear property is required to maintain the design contour during long-term running. However, the latest engines are endeavoring to fully atomize the spraying fuel for the purpose of sufficient burning. This trend stimulates researches for improving the wear resistance of the cam-roller to satisfy the requirements of higher pumping pressure. Johnston [1] adopted the diamond-like carbon (DLC) coating to lower the wear rate of cam-shim surface. Malatji [2] found Zn-5 g/L Al_2O_3 nanocomposite coating possessed the highest corrosion resistance and lowest wear loss. Chernyshev [3] employed the arc remelting method to make a hardened layer on the cast iron cam surface with 0.64–1.4-mm thickness and 50–54-HR_C hardness. The above studies promoted anti-wear property by surface modifying, which is also the main surface strength method up until now. Another roadmap is the active surface topography optimization [4], namely the surface texturing. The textured surface contains vast regular micro-structures serving as the hydrodynamic bearings or micro-traps for wear debris [5]. It also can transform the lubrication condition from a high-friction boundary to a lower friction mixed regime [6]. It has been successfully applied in various subjects, such as piston rings [7], cylinder liner [8], and cutting tools [9, 10].

Surface texturing has the compatibility with both conformal contact and nonconformal contact [11]. The beneficial effects on conformal contacts have been well established; however, the lubrication mechanism in nonconformal contact have not been fully revealed [12–14]. Jacobson [15] first indicated the surface

morphology plays a crucial role in nonconformal contact. After that, Wang et al. [11] found that the optimal texture exists for a specific cylinder radius in line contact. Surface morphologies trap the lubricant and maintain the lubricity for the repeated start-ups and stops of motions [16]. For the point contact, Segu [12] investigated the friction properties of combined texture surface. A transition from the boundary to mixed lubrication regime was observed and that causes a lubrication effect. Krupka [14] found that the depth of micro-dimples was critical, since it highly related to the film thickness.

The contact of running cam-roller is a typical nonconformal (line) contact. Therefore, the surface texturing technology is very promising to reduce the wear and improve lubrication. Also, some early studies [17, 18] have revealed the surface strengthening of laser treatment, while this effect has not been researched with surface morphology, namely surface texturing, compatibly and systematically. On the other hand, a cam's wear mainly distributes in the lifting region due to the higher pressure and motion speed in this region. In this case, the directivity of laser machining turns to extremely important. By only laser machining the local region, it is possible to avoid the deformation and redundant strengthening generated by the integrated heat treatment of camshaft. More importantly, a serial of the aided processes of heat treatment, including straightening, surface precision grinding, and polishing could be simplified or even removed, companying with a lower cost in manufacturing.

The motivation of this study was to investigate the benefits of the laser surface texturing on tribological performance of injection cam. Specifically, the tribological experiment was carried out on a line contact tester. After that, the LST injection cams were made and their anti-wear performance was explored by a single-cylinder diesel engine. The engine's performance was monitored during the 300-h bench test. The cams' wear were analyzed by lifting loss curves.

Table 1 Parameters of laser system

Parameters	Value range
Repetition frequency	0.1–20 kHz
Max average power	10 W
M^2 factor	≤2
Beam diameter	3 mm
Laser beam expanders	3 times
Focal length	60 mm
Spot diameter	60 μm

2 Experimental details

Laser surface texturing (LST) is an approach to obtain the controllable and precise surface texturing. Besides the lubrication effect, LST process can also influence the surface property of the processing target. The authors have employed solid laser source for surface texturing and strengthening for many years. In this study, the laser source was the CEO® REA series, 150-watt Nd:YAG with extra cavity doubled and output 532-nm wavelength, green light Q-switched pulsed laser. Contrasting to the 1064-nm wavelength or continuous wave laser, this laser source has less heat effect on the metallic material surface [19]. Hence, the generation of recast layer is restrained effectively. Table 1 lists the specific parameters of the laser system in this study.

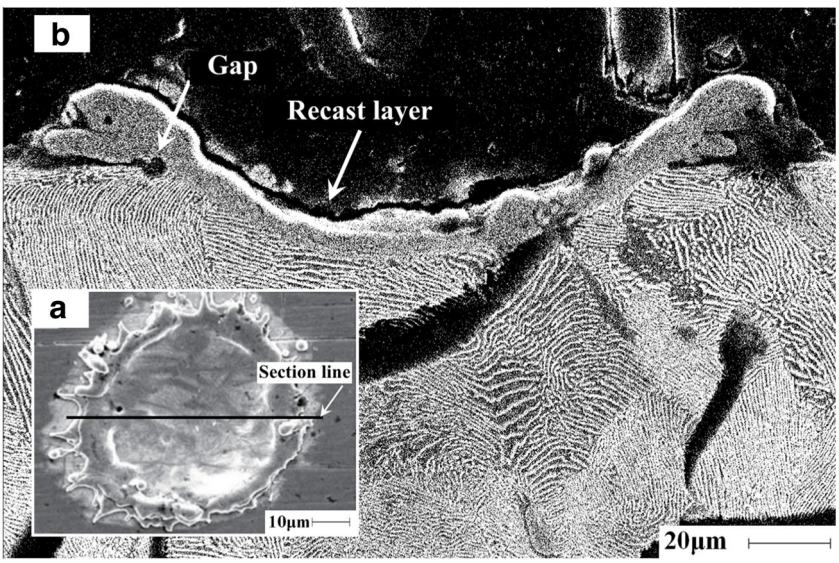

Fig. 1 The view of single dimple. **a** Vertical morphology view. **b** Metallograph of cross-section view

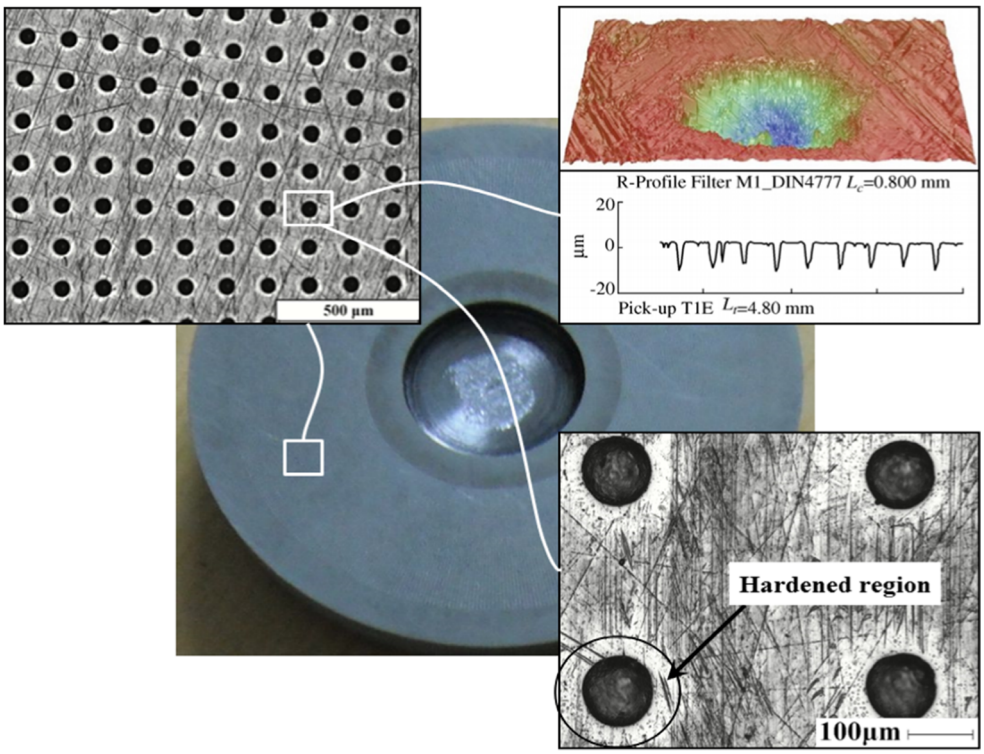

Fig. 2 Textured specimen and local area's micrographs

Figure 1 depicts the metallograph of single textured dimple on the cast iron surface. From the vertical view (Fig. 1a), it can be seen that the LST process generates a remelting layer around the texture morphology in a continuous flow form. It indicates that the LST process in this study is able to modify the surface morphology and material property of the local region simultaneously. From the cross-section view (Fig. 1b), it is evident that the remelting layer includes the bulge part and the sub-surface part. The combination of bulge part and base material is unstable since a gap exists between them. These features are conducive to amend the surface flatness (remove the recast bulge) after LST treatment.

Figure 2 shows the textured specimen (nodular cast iron) and the micrographs of local area's morphologies. The specimen was textured firstly and then polished by 200#, 600#, and 800# sand papers successively. After polishing, it can be seen that bulge part of remelting layer was removed completely. The surface hardness of the hardened regions, the bright areas produced by LST treatment was 750–850 HV, nearly two times higher than the un-textured area, surface hardness 400–450 HV. In addition, the dimple depths before and after polishing were characterized by the white light interferometry microscope, respectively. The effect of the polishing process on the dimple's depth was less than 1 μm; therefore, this deviation was ignored later on. The profile curve of a column dimple showed that the consistency of texture morphologies was acceptable also.

The effect of laser surface remelted treatment on the anti-wear property was studied by Bylica and Adamiak [17], who found that abrasive resistance of laser-hardened samples was about six times higher than that of normalized samples. Molian and Baldwin [18] also found that laser-hardened gray and ductile cast iron's wear resistance were positively related with the depth of the hardened layer. In this study, the laser beam just remelted a partial region of the whole surface and the depth of the remelted layer was also limited; hence, the surface hardness of it was inferior to the previous processes. However, the LST surface owns the combined advantages of lubrication effect and local hardening, so what about the anti-wear property of it?

The experiment included two parts. First, the performance of textured surface was investigated on the tribological tester. The previous studies showed that dimple depth, area density, and movement speed are crucial for lubrication [8, 14], therefore a three-factor experiment, each factor has five levels (see Table 2), was established. The area density of micro-dimple array was controlled by the same equal space in row and

Table 2 Parameters of tribological experiment

Parameters		Values
Diameter, d	[μm]	70
Area density, ρ	[%]	0, 3, 10, 17, 40
Depth, h	[μm]	0, 5, 8, 12, 24
Rotation speed, ω	[r/min]	80, 150, 220, 300, 400

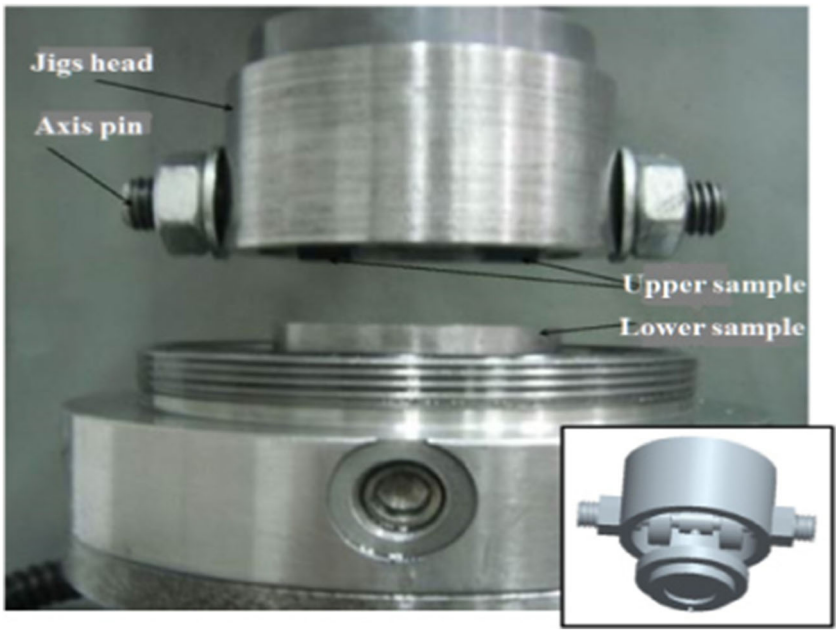

Fig. 3 Tribological tester and its drawing entity

column directions. The intervals of area densities 3, 10, 17, and 40% were 700, 400, 300, and 200 um, respectively. The characterization of surface textures referred to the existing system [20]. Every specimen experienced the continuous increasing of rotation speed from 80 to 400 r/min. Each rotation speed had the same operation time, 30 min. The result of the friction coefficient at certain rotation speed was the average value of a stabilized period time.

Figure 3 shows the structure of tribological tester. The upper sample (two small rings, surface roughness Ra 0.2–0.3 μm) was assembled on an axis pin with the rotation degree of freedom only. The axis pin was further fixed on the jig's head, which was connected to the live spindle. The lower sample, where the surface texturing was processed, remained still during the test. Below it, a dynamical sensor measured the friction torque. The friction coefficient between upper and lower samples was calculated by the computer automatically and dynamically. The contact load produced by a precise spring was loaded steadily on the lower sample. The above mechanism simulated the cam-roller friction pair's motion and contact. The diameter of the upper sample referring to the real roller was 20 mm. It was rotating and sliding on the lower sample surface as the live spindle spinning. The material of

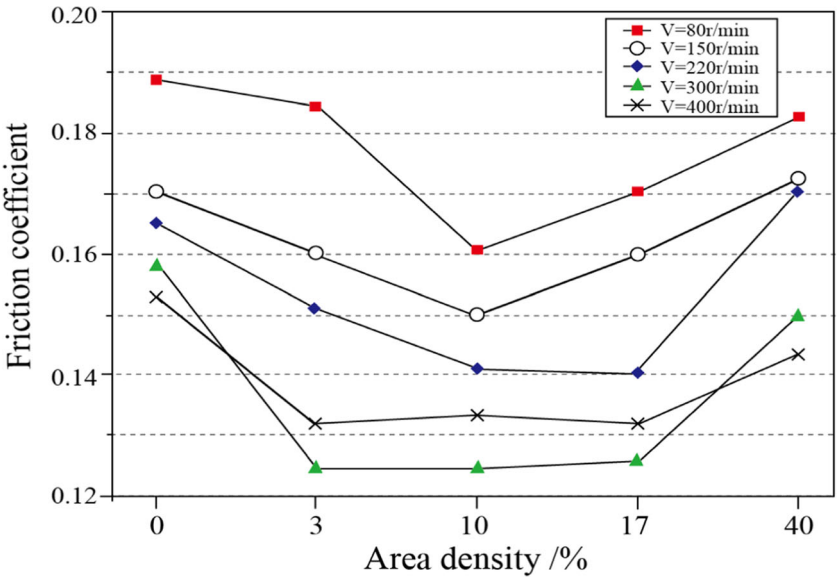

Fig. 4 Effect of area density on the friction coefficient at various rotation speeds, $h = 8$ μm

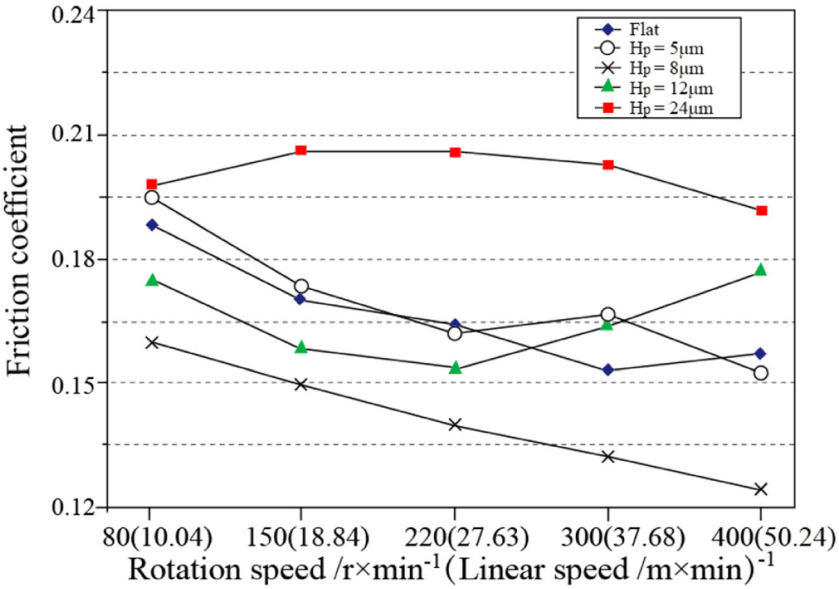

Fig. 5 Effect of relative movement speed on the friction coefficient at various dimple depth, $\rho = 10\%$; the x-coordinate contains rotating speed and equivalent linear speed

upper sample was AISI 1045 steel with a nominal hardness of 55–60 HR_C. The lubricant, SAE15W/40 (dynamic viscosity 172.4 mPa·s at 20 °C), was sufficiently applied during the experiment.

After the tribological experiment, we found it was challenging to estimate the actual wearing capacity of the worn specimens. On the one hand, the mass loss did not reflect the real wear degree, not only because the runtime was very

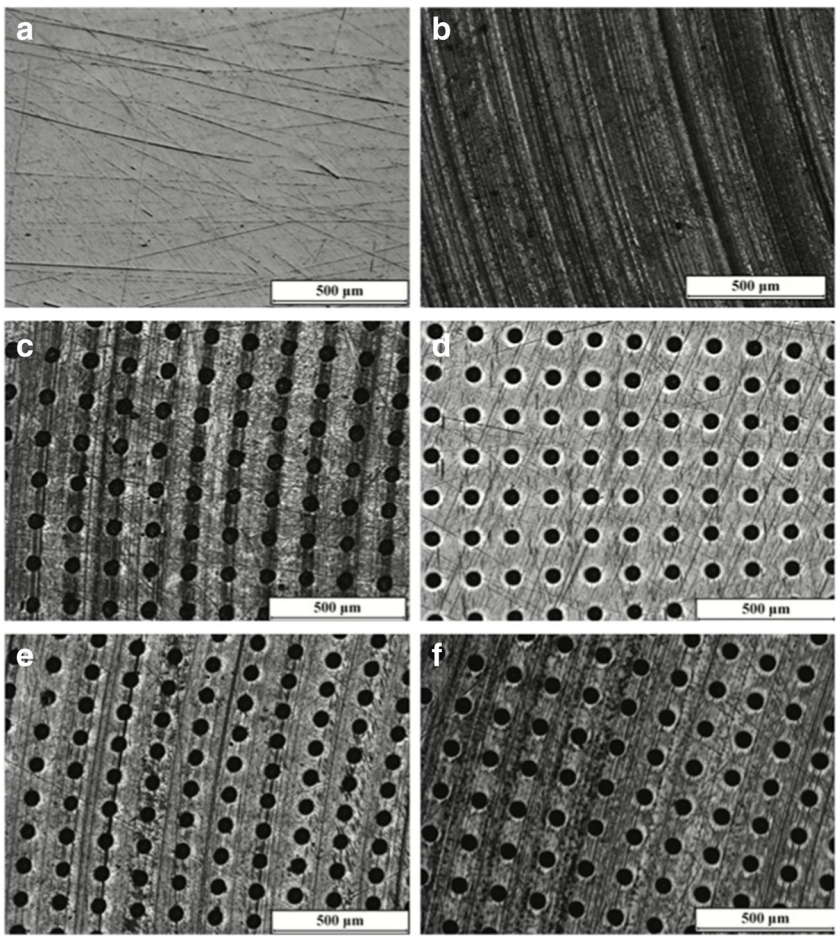

Fig. 6 Worn surfaces with $S_p = 10\%$ and various dimple depths. **a** Flat. **b** Flat and worn. **c** $h = 5$ μm. **d** $h = 8$ μm. **e** $h = 12$ μm. **f** $h = 24$ μm

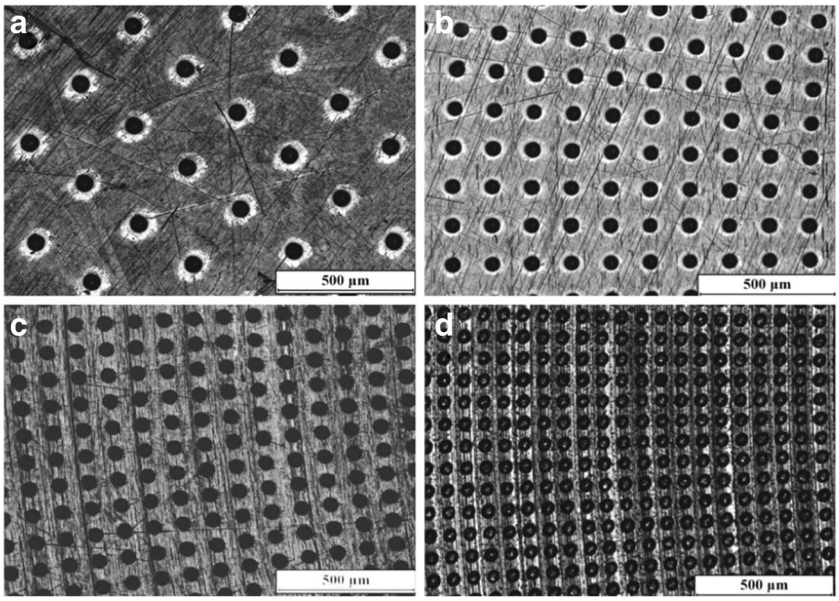

Fig. 7 Worn surfaces with $h = 8$ μm and various area densities. **a** $S_p = 3\%$. **b** $S_p = 10\%$. **c** $S_p = 17\%$. **d** $S_p = 40\%$

limited but also the adhesive wear transferred material between upper and lower samples. On the other hand, since the scratched occurred randomly and heavily, the wear characterization through the surface parameters was also inaccurate. For the above reasons, this part of the work compared the wear degrees qualitatively and roughly by the micrographs of worn surface.

To further investigate the anti-wear property of LST cam, the engine test was carried out on a single cylinder diesel engine with referencing the results of tribological experiment. The main parameters of tested engine were as follows: cylinder diameter 105 mm, stroke length 120 mm, displacement 1.039 L, compression ratio 17, rated power 11 KW, and rated speed 2200 r/min. The material of the roller was bearing steel GCr15 with surface hardness 58~63HR_C.

The bench test was conducted continuously at rated power and speed for 300 h. The LST was processed on the lifting region of oil injection cam surface. All throughout the test, the engine's performance was monitored and the curves of cams' lifting loss were obtained lastly to investigate the influence of LST to the cams' controlling accuracy.

3 Results and discussion

3.1 Tribological experiment

Figure 4 shows the effect of area density on the friction coefficient at various rotation speeds with 8-μm dimple depth and 100 N load force. Under all the rotation speed conditions, the curves of friction coefficient had the similar trend of fluctuation. As the area density of LST ranged from 0 to 10%, the friction coefficient decreased accordingly, while in the range of 10 to 40%, the friction coefficient had an upward trend. Therefore, for all the movement speeds, the optimum area density was about 10%. Noting the value range of optimum area density was extending along with the rising of rotation speed, which means LST was more compatible with high speed.

Figure 5 shows the effect of dimple's depth on the friction coefficient at various rotation speeds. The area density was 10% and load force was 100 N. It can be observed that the deepest dimple (24 μm) had the highest level of friction coefficient, while the dimples with 8-μm depth obtained the lowest friction. On the other hand, the friction coefficient curve had a downward trend as the rotation speed increased, which agreed with the previous studies [11, 15]. The main reason was that the relative velocity and film thickness are relevant on the condition of EHL [12]. The upper and lower samples were under mixed lubrication at the lower speed and the reinforced lubrication could depart two surfaces and result in friction reduction as the speed increased.

Table 3 Parameters of LST cams

Camshaft no.	Dimple depth	Area density
0#	–	–
1#	8 μm	10%
2#	8 μm	17%

Figures 6 and 7 show the OM images of the worn specimens. It can be seen that fewer wear tracks existed on the low friction coefficient specimens. For the h = 8 μm and ρ = 10% specimens, their surface wear tracks were unapparent, which means that the film thickness was increased and direct contact of two surfaces was avoided significantly. Compared to the flat specimen, the textured specimen with 40% area density (Fig. 7d) showed more severe wear on it. This result indicated that the improper surface texture might have a negative effect on the lubricant film formation. Reasons might be that the reduction of surface bearing capacity roughed surface and increased the microcontact pressure.

The above experiment result was similar to the [21], which found that the 200-μm diameter dimples with 10% area density exhibited the highest wear resistance on the ball-on-disk tester. Differently, Ref. [22] indicated that high area density (higher than 6%) was harmful to wear resistance. Therefore, in-depth studies are still needed for the specific object and goal.

3.2 Three hundred hours of engine test

The tribological experiment indicated that the surface texturing with certain area density and depth has the best performance in friction reduction. Plus, the wear is one of the ultimate embodiments of the surface friction; it can be estimated that the low friction texture pattern may also have a positive effect on the anti-wear property. Hence, the texture patterns of following engine test were S_p = 10% or 17%, h = 8 μm, and d = 70 μm (see Table 3). The LST processed the cams' lifting region only, where the severe wear often happens.

Three camshafts with different LST area densities were tested separately on a same engine. Figure 8 shows the design roller displacement of the tested injection cam. The lifting angle of camshaft was from 90° to 150°, the corresponding region on the cam surface was LST processed to promote its anti-wear property. The engine test was conducted at rated power and speed for 300 h. In every installation, the engine oil was changed and all the moving parts were examined to ensure the same condition. During the test, the engine showed the same performance in output power and fuel consumption. It means that the lubricity of cam-roller follower can hardly influence the engine's performance, since it is not the main source of friction loss in the engine [23].

After 300 h running, three camshaft surfaces were 3D characterized at three different representative angles in the lifting region, 100° (initial point), 125° (center point), and 150° (terminal point), as shown in Fig. 8. Their 3D surface morphologies and section profiles (along with the white dash lines) are shown in Fig. 9. The wear depths could be estimated by analyzing the change of dimples and the number of wear tracks. Above all, two textured schemes promoted cam's wear resistance differently.

In the angle 100°, the obvious wear tracks and remaining hardened regions could be observed in all three camshafts, for instance a 5 μm depth wear trace appeared on no. 0#. The possible reason for this feature could be the roller displacement rose rapidly around this point, generating impact load on the cams' local surface. The rest of the dimple depths of 1# cam and 2#

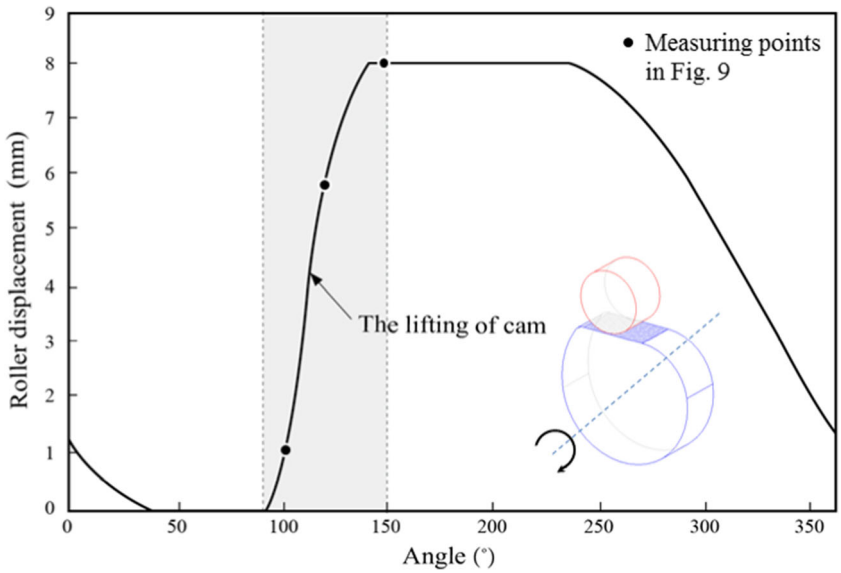

Fig. 8 Datum displacement graph of the pump cam

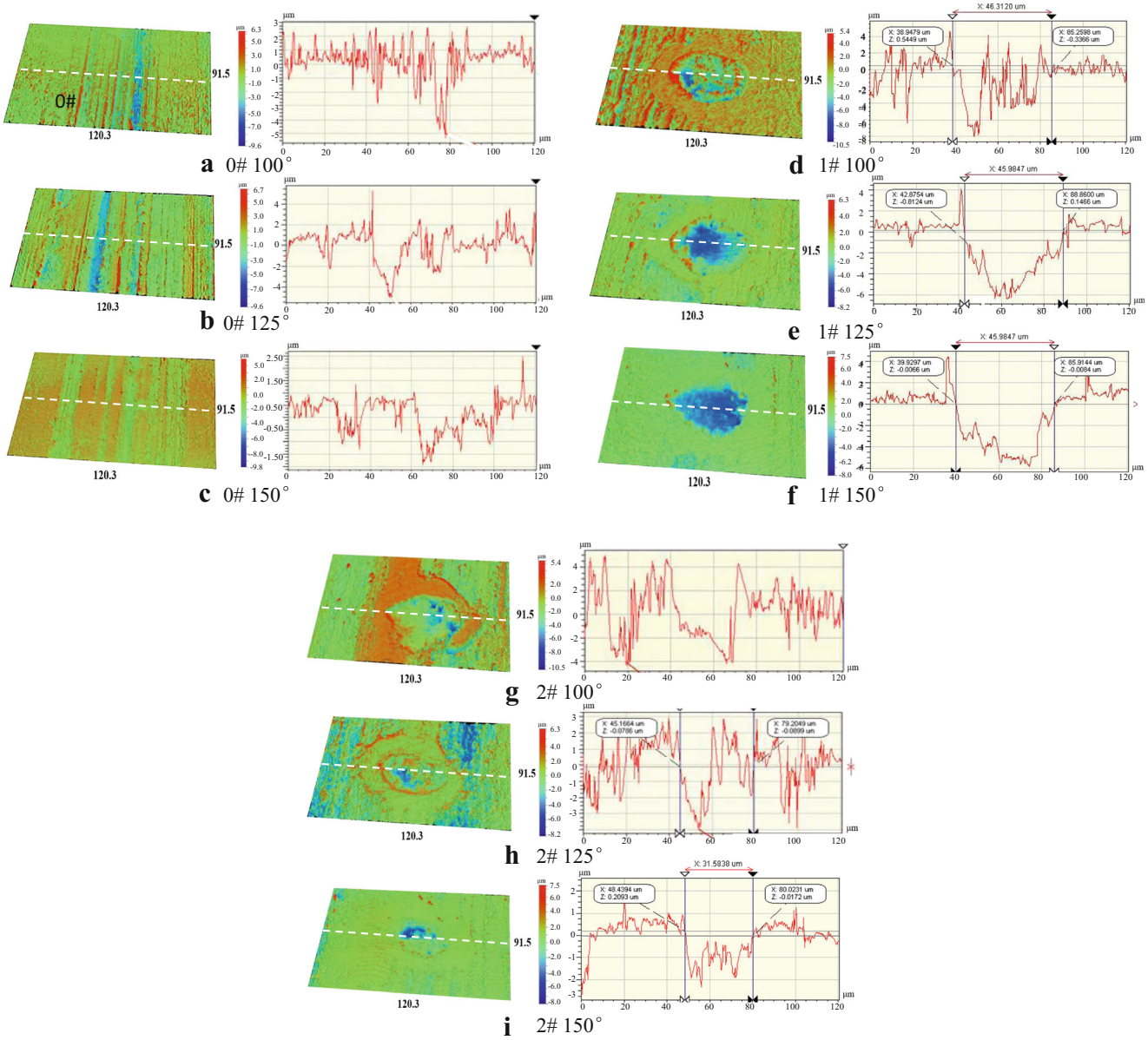

Fig. 9 3D surface morphologies of camshafts at three different angles, the sample points located in the middle of cams' width. **a**–**c** Camshaft 0#. **d**–**f** Camshaft 1#. **g**–**i** Camshaft 2#; section profiles along with the *white dash lines*

cam were about 4 μm, while only the latter showed an integrated section profile, indicating a better wear resistance ability. In the angle 125°, the decreased lifting velocity and load reduced the number of tiny wear tracks on the non-textured cam (0#); meanwhile, 1# cam showed the slightest wear traces, while 2# cam showed little promotion in wear resistance. In the angle 150°, the lifting stage was finished, while the cam-roller reached their highest contact pressure. Therefore, depth loss and shallow wear trace could be still observed in Fig. 9a, i, respectively, noting that dimple depth loss of 1# cam was only 2 μm.

Figure 10 shows the cam lifting loss curves of camshaft no.1–3 after 300 h operation. The single point in cam lifting loss curve reflects the lifting displacement loss (difference value) at certain angle. The area of the region bounded by cam lifting loss curves, S, reflects the cams' accuracy. S_0 for the 0# cam was 0.354, S_1 for the 1# cam was 0.249 and S_2 for

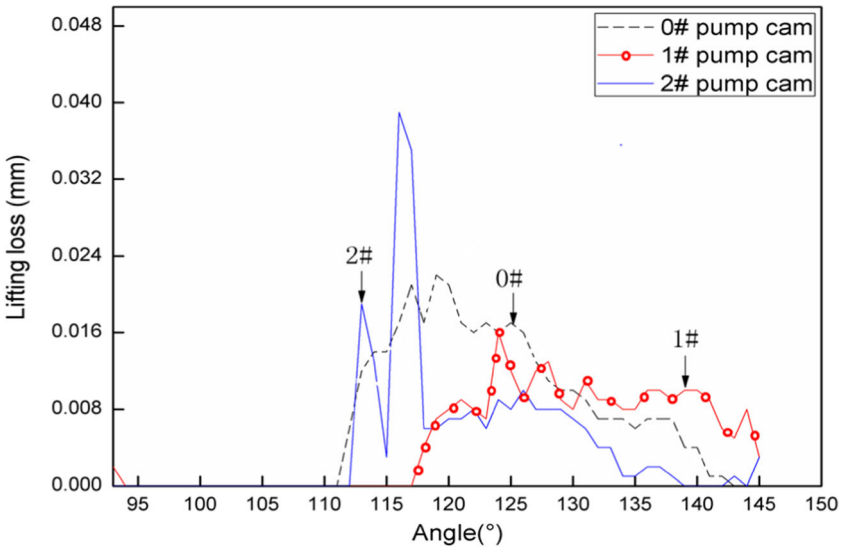

Fig. 10 Cams' lifting loss curves

the 2# cam was 0.232. From the above results, the two LST injection cams both showed the promotion of controlling accuracy after longtime running. Another feature realized, was that these two cams have different lifting loss distributions around their contours. The 2# cam had the minimum lifting loss, 34.4% reduction compared to the 0# cam (original) and its distinct lifting loss appeared in the range of angle 110°–120°. The overall wear of the 1# cam decreased by 29.7% and its distribution of lifting loss was more uniform comparing to the others.

Combining with Figs. 9 and 10, an obvious feature was that the changes of surface micro-morphology did not match the macro-loss of the rollers' displacement. Actually, the latter was far more than the former in all cases. Therefore, it could be concluded that the plastic deformation was also a source of lifting loss and it was highly affected by the textured area density. For instance, higher area density texture (17%, 2# cam) showed a negative effect on contour accuracy in the range of angle 110°–120°.

For the metal material, laser processes can be classified into three types mainly: vaporization, melting, and non-melting. For the melting and non-melting processes, laser beams strengthen the surface material by the grain refinement (size reduction) mechanism [24]. The laser source adopted in this study has a combination effect of vaporization and melting. These two effects generate the micro-dimple and remelting layer on the cams surface, both of which contribute to promoting the anti-wear property. From the above experimental results, it can be concluded that the main function of surface texturing is to enhance the lubricity by the optimum design without weakening the surface strength.

4 Conclusions

In this study, LST was introduced to the injection cams' surface to promote its anti-wear property. The experiment result will contribute to the cams' surface design and manufacturing. The following conclusions can be drawn from the experimental investigation:

(1) In the LST process, the laser beam increases the local regions' hardness 2–3 times by the remelting process. This feature promotes the wear resistance of cam surface together with the lubrication effect of surface texturing; therefore, some degree of laser heat effect is beneficial.
(2) In the tribological experiment, the textured specimen having a dimple density of about 10% and a dimple depth of about 8 μm showed a promotion in lubrication, especially in the high speed working condition.
(3) The 300 h engine test showed an agreement with the tribological experiment, which also indicated that the anti-wear property of LST cams increased nearly 30% compared to the un-textured cam. The non-uniform distribution of lifting loss was observed, it shows the importance of maintaining the cams' surface bearing ratio in surface texturing design.

Acknowledgments This work was financially supported by the National Natural Science Foundation of China (51175233), the Innovation Project for Graduate Student Research (KYLX15_1048) and Technology project (BE2016144, 2015095) of Jiangsu province.

References

1. Johnston SV, Hainsworth SV (2005) Effect of DLC coatings on wear in automotive applications. Surf Eng 21(21):67–71
2. Malatji N, Popoola API, Fayomi OSI, Loto CA (2016) Multifaceted incorporation of Zn-Al_2O_3/Cr_2O_3/SiO_2 nanocomposite coatings: anti-corrosion, tribological, and thermal stability. Int J Adv Manuf Technol 82(5):1335–1341
3. Chernyshev AN, Kaplina IN, Serapin MI (1996) Surface hardening with remelting of functional surfaces of cast iron camshafts. Metal Science and Heat Treatment 38(10):440–442
4. Cabanettes F, Claret-Tournier J, Mohlin J, Nilsson PH, Rosén BG (2009) The evolution of surface topography of injection cams. Wear 266:570–573
5. Etsion I (2004) State of the art in laser surface texturing. J of Trib 127(1):761–762
6. Kovalchenko A, Ajayi O, Erdemir A, Fenske G (2011) Friction and wear behavior of laser textured surface under lubricated initial point contact. Wear 271(9):1719–1725
7. Etsion I, Sher E (2009) Improving fuel efficiency with laser surface textured piston rings. Tribol Int 4254:2–7
8. Grabon W, Koszela W, Pawlus P, Ochwat S (2013) Improving tribological behaviour of piston ring-cylinder liner frictional pair by liner surface texturing. Tribol Int 61:102–108
9. Kawasegi N, Sugimori H, Morimoto H, Morita N, Hori I (2009) Development of cutting tools with microscale and nanoscale textures to improve frictional behavior. Precis Eng 33(3):248–254
10. Ma J, Duong NH, Lei S (2015) 3D numerical investigation of the performance of microgroove textured cutting tool in dry machining of Ti-6Al-4V. Int J Adv Manuf Technol 79(5):1313–1323
11. Wang X, Liu W, Zhou F, Zhu D (2009) Preliminary investigation of the effect of dimple size on friction in line contacts. Tribol Int 42(7): 1118–1123
12. Segu DZ, Kim SS (2014) Influence on friction behavior of micro-texturing under lubricated non-conformal contact. Meccanica 49(2):483–492
13. Sudeep U, Tandon N, Pandey RK (2015) Performance of lubricated rolling/sliding concentrated contacts with surface textures: a review. J of Trib 137(3):031501 1–11
14. Křupka I, Hartl M (2007) The effect of surface texturing on thin EHD lubrication films. Tribol Int 40(7):1100–1110
15. Jacobson B (2000) Thin film lubrication of real surfaces. Tribol Int 33(3):205–210
16. Zhao J, Sadeghi F (2004) The effects of a stationary surface pocket on EHL line contact start-up. J of Trib 126(4):672–680
17. Bylica A, Adamiak S (2002) Laser bean hardening of carbon steels. Archives of foundry 2(6):43–53
18. Molian PA, Baldwin R (1968) Wear behavior of laser surface hardened gray and ductile cast irons. Part 1—sliding wear. J of Trib 108:326–333
19. Knowles MRH, Rutterford G, Karnakis D, Ferguson A (2007) Micro-machining of metals, ceramics and polymers using nanosecond lasers. Int J Adv Manuf Technol 33(1): 95–102
20. Kang ZY, Fu YH, Ji JH, Wang H (2015) Characterisation of group behavior surface texturing with multi-layers fitting method. Nondestruct Test Eva 31(3):235–246
21. Tripathi K, Joshi B, Gyawali G., Amanov A, Lee SW (2015) A Study on the effect of laser surface texturing on friction and wear behavior of graphite cast iron. J of Trib 138(1):011601 1–10
22. Koszela W, Dzierwa A, Galda L, Pawlus P (2012) Experimental investigation of oil pockets effect on abrasive wear resistance. Tribol Int 46(1):145–153
23. Taylor CM (1998) Automobile engine tribology-design considerations for efficiency and durability. Wear 221(1):1–8
24. Gualtieri E, Borghi A, Calabri L, Pugno N, Valeri S (2009) Increasing nanohardness and reducing friction of nitride steel by laser surface texturing. Tribol Int 42:699–705